IOPscience

Home   Search   Collections   Journals   About   Contact us   My IOPscience

Multimodel uncertainty changes in simulated river flows induced by human impact

parameterizations

This content has been downloaded from IOPscience. Please scroll down to see the full text.

Multimodel uncertainty changes in simulated river flows induced by human impact parameterizations

Xingcai Liu[1], Qiuhong Tang[1,2], Huijuan Cui[3], Mengfei Mu[1,2], Dieter Gerten[4], Simon Gosling[5], Yoshimitsu Masaki[6#], Yusuke Satoh[7], Yoshihide Wada[7,8,9,10]

[1]Key Laboratory of Water Cycle and Related Land Surface Processes, Institute of Geographical Sciences and Natural Resources Research, Chinese Academy of Sciences, Beijing 100101, China

[2]University of Chinese Academy of Sciences, Beijing 100101, China

[3]Key Laboratory of Land Surface Pattern and Simulation, Institute of Geographical Sciences and Natural Resources Research, Chinese Academy of Sciences, Beijing 100101, China

[4]Potsdam Institute for Climate Impact Research, 14412 Potsdam, Germany & Humboldt-Universität zu Berlin, Unter den Linden 6, 10099 Berlin, Germany

[5]School of Geography, University of Nottingham, Nottingham NG7 2RD, United Kingdom

[6]National Institute for Environmental Studies, 16-2 Onogawa, Tsukuba, Ibaraki, 305-8506, Japan

[7]International Institute for Applied Systems Analysis, Laxenburg, Austria

[8]NASA Goddard Institute for Space Studies, New York, USA

[9]Center for Climate Systems Research, Columbia University, New York, USA

[10]Department of Physical Geography, Utrecht University, Utrecht, The Netherlands

Corresponding author: Qiuhong Tang (tangqh@igsnrr.ac.cn)

[#] Current address: Graduate School of Science and Technology, Hirosaki University, Bunkyocho-3, Hirosaki, Aomori, 036-8561, Japan.

1   **Abstract**

2   Human impacts increasingly affect the global hydrological cycle and indeed dominate

3   hydrological changes in some regions. Hydrologists have sought to identify the human-impact-

4   induced hydrological variations via parameterizing anthropogenic water uses in global

5   hydrological models (GHMs). The consequently increased model complexity is likely to

6   introduce additional uncertainty among GHMs. Here, using four GHMs, between-model

7   uncertainties are quantified in terms of the ratio of signal to noise (SNR) for average river flow

8   during 1971-2000 simulated in two experiments, with representation of human impacts

9   (VARSOC) and without (NOSOC). It is the first quantitative investigation of between-model

10   uncertainty resulted from the inclusion of human impact parameterizations. Results show that

11   the between-model uncertainties in terms of SNRs in the VARSOC annual flow are larger

12   (about 2% for global and varied magnitude for different basins) than those in the NOSOC,

13   which are particularly significant in most areas of Asia and northern areas to the Mediterranean

14   Sea. The SNR differences are mostly negative (-20% to 5%, indicating higher uncertainty) for

15   basin-averaged annual flow. The VARSOC high flow shows slightly lower uncertainties than

16   NOSOC simulations, with SNR differences mostly ranging from -20% to 20%. The uncertainty

17   differences between the two experiments are significantly related to the fraction of irrigation

18   areas of basins. The large additional uncertainties in VARSOC simulations introduced by the

19   inclusion of parameterizations of human impacts raise the urgent need of GHMs development

20   regarding a better understanding of human impacts. Differences in the parameterizations of

21   irrigation, reservoir regulation and water withdrawals are discussed towards potential directions

22   of improvements for future GHM development. We also discuss the advantages of statistical

23   approaches to reduce the between-model uncertainties, and the importance of calibration of

24   GHMs for not only better performances of historical simulations but also more robust and

25   confidential future projections of hydrological changes under a changing environment.

26

27   Keywords: Uncertainty; Global hydrological model; Human impact parameterizations;

28   Multimodel approach;

29

1. Introduction

31　　Human activities have greatly affected the hydrological cycle [1, 2], whereas the

32　simulation of human water uses and model uncertainties therein are still great challenges for

33　global hydrological modeling [3]. Model simulations have shown that discharge has been

34　increasingly disturbed by human water uses in the late 20th century [4]. In the recent decade,

35　hydrologists have made large efforts to identify the human impacts on hydrological cycle under

36　a changing environment [5-11]. The major human impacts (e.g. irrigation and reservoirs) have

37　been more or less parameterized in many global hydrological models (GHMs) [12-18].

38　　However, large discrepancies among models result from the differences in model input,

39　algorithms, parameters, etc. [3, 19]. The parameterizations of human impacts vary greatly

40　across GHMs and thus possibly bring extra discrepancies among models. Hydrologists are

41　aware of the uncertainties among GHMs and some intercomparison projects have been

42　initialized to profile them. For example, the between-model uncertainties for naturalized

43　simulations of GHMs have been investigated through the Water Model Intercomparison Project

44　(WaterMIP) [20] and the Inter-Sectoral Impact Model Intercomparison Project (ISIMIP) Fast-

45　track [21, 22]. The human water uses such as irrigation are remarkable in some regions with

46　intensive human impacts (e.g. western United States, China, and South Asia), and can induce

47　considerable uncertainties in hydrological projections for the future [9, 23]. All these prior

48　studies showed large discrepancies among GHMs in future hydrological projections, however,

49　these uncertainties might result from numerous differences among GHMs, e.g., different input

50　data and model algorithms, which makes it difficult to clarify the uncertainty sources. The

51　ISIMIP phase 2 provides a framework for comparing and evaluating multiple GHMs based on

52　consistent input data, e.g., meteorological forcings, human impacts (reservoirs and irrigation

53　area), and drainage network for flow routing. In view of the potential influence of human

54　impacts on the GHMs simulations, it is now possible to examine the changes of between-model

55　uncertainty induced by the inclusion of human impacts in GHMs quantitatively, based on the

56　ISIMIP2 simulation protocol.

57　　In this study, we use four GHMs to investigate the uncertainty changes in the simulations

58　with and without human impact parameterizations. On this basis, we further provide discussions

59 on the differences in the parameterization of human impacts, which are associated with

60 between-model uncertainties. This paper is organized as follows: description of models,

61 experiments and methods are presented in Section 2; results are presented in Section 3; the

62 implications of the results are discussed in Section 4 and a summary is presented in Section 5.

63

2. Data and Methodology

2.1. Models and experiments

66 River flow simulations from four GHMs, i.e. DBH [24-26], H08 [12, 27], LPJmL [28, 29],

67 and PCR-GLOBWB [30, 31], forced by four meteorological forcing data, namely Princeton

68 [32], GSWP3 [33] (http://hydro.iis.u-tokyo.ac.jp/GSWP3/), WFDEI [34] and WATCH [35], for

69 the historical period 1971-2000 are used in this study. A description of the models is given in

70 Table S1. Two experiments were conducted for all GHMs and forcings: (1) simulations under

71 natural condition without human impacts (i.e., naturalized simulations, refer to NOSOC) and

72 (2) simulations with human impacts including irrigation and reservoir regulation, which is

73 related to varied socioeconomic information (refer to VARSOC).

2.2. Human impacts in GHMs

75 In the experiment, human impacts are considered in terms of irrigation and reservoir

76 regulation. Time-varying areas of both irrigated and rainfed cropland are represented as the

77 combination of present-day (year 2000) areas of crop types from MIRCA2000 [36] and

78 backward trends of agricultural land cover from HYDE [37]. The reservoir (dam) information

79 is derived from the Global Reservoir and Dam (GRanD) Database [38], with the locations re-

80 arranged to half-degree grid cells based on the global drainage direction map (DDM30) [39].

81 The reservoirs are included or not for regulation according to the documented year of

82 completion. Reservoirs and irrigation areas used in the experiment are shown in Figure S1. The

83 river basin delineations defined by the DDM30 data [39] are used for analysis at basin scale.

84 The parameterizations of human impacts in the four GHMs are summarized in Table S1 by

85 referring to the relevant literature and Table 1 in Ref. [9] and [30], who have documented the

86 human water uses in several state-of-the-art GHMs specifically including those used here.

2.3. Uncertainty measurement

Streamflow simulations from the experiment with human impacts are compared with the observed station data from the Global Runoff Data Centre [40] to evaluate the performances of GHMs. Annual flow (*AF*) and highest monthly flow (*HMF*) for each year, and their means over the study period, i.e. mean annual flow (*MAF*) and mean highest monthly flow (*MHMF*) are computed. Relative errors between simulated and observed MAF and MHMF, and the correlation coefficients between simulated and observed AF and HMF are calculated for each station. The respective simulated streamflow is picked out from the global grids according to the latitudes and longitudes of stations. The stations (1235 in total) with record lengths of more than 20 years and catchment areas larger than 10,000 km^2 are used for comparison (see Figure S2).

The signal to noise ratio (SNR), defined as the mean divided by the standard deviation, is used as an indicator of uncertainty among the multimodel simulations. SNR is calculated for global and basin-averaged MAF and MHMF from model grid cells to address the uncertainty in the simulations with and without human impacts. SNR differences between the experiments with and without human impacts are interpreted as the change of uncertainty caused by the inclusion of human impacts in GHMs. Annual SNR is also computed for global AF and HMF for temporal change analysis during the 1971-2000 period.

3. Results

3.1. Evaluation of GHMs

Figure 1 shows the observed MHMF (Figure 1a) and MAF (Figure 1b) versus the ensemble means of simulations across all GHM-forcing combinations. Both MHMF and MAF simulations show large deviations at many stations with relatively small catchment areas, while stations with large catchment areas tend to show little deviation. For the ensemble means, about 10% of the stations show small relative errors of -10% to 10%, while more than 40% of stations show relative errors of -50% to 50% for both MHMF and MAF. For the ensemble of individual GHM, no more than 10% (15%) of stations show small relative errors of -10% to 10% for MHMF (MAF), and about 20% to 30% have relative errors of -50% to 50% for both MHMF

116   and MAF (see Table S2). The simulations of MAF show generally better performance than

117   those of MHMF at most stations, but both of them seem to be overestimated at many stations.

118   The correlation coefficients between the simulated and the observed HMF and AF are

119   shown in Figure 1c. The correlation coefficients for AF are significantly larger than those for

120   HMF. Nearly 70% (85%) stations have correlation coefficients greater than 0.6 for HMF (AF).

121   The proportions are larger than those for individual models (see Table S3). This brief evaluation

122   indicates that improvements of GHMs are necessary to capture river flows, particularly in small

123   catchments, and ensemble means of multimodel simulations usually fit better to observations.

124
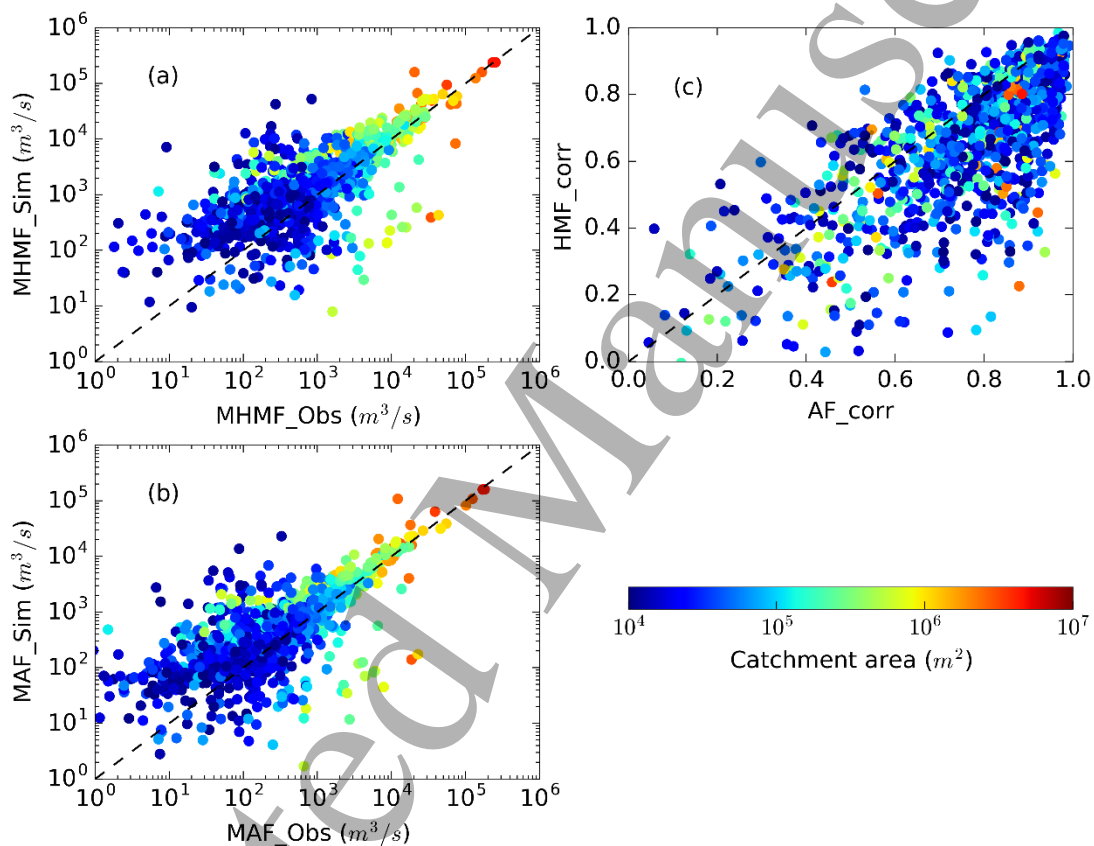
125   Figure 1. Evaluation of the ensemble discharge means across all GHM-forcing combinations with GRDC

126   observations: (a) ensemble means of simulated (MHMF_Sim) versus observed MHMF (MHMF_Obs),

127   (b) ensemble means of simulated (MAF_Sim) versus observed MAF (MAF_Obs), (c) correlation

128   between simulated and observed HMF (HMF_corr) versus correlation between simulated and observed

129   AF (AF_corr). The colors of data points indicate the catchment areas of hydrological stations.

130

131   **3.2. Uncertainty assessment**

132   Figure 2 shows the SNRs for the experiment with human impacts and the SNR differences

133   between the experiments with and without human impacts for global HMF and AF. During the

134   1971-2000 period, the all-ensemble SNR of global HMF ranges from 4 to 5, and SNR of global

135   AF ranges from 4.5 to 5.5. SNRs show large spread among different meteorological forcings

136   (see Figure 2a, c): the WATCH's SNR is the smallest (~4 for HMF and 4.5-5 for AF) over the

137   historical period; WFDEI's SNR shows the same value as WATCH's before 1979 (WFDEI and

138   WATCH share the same data for this period) and then increases greatly to be the largest (~5.5

139   for HMF and ~7.5 for AF) among those of the four forcings; the PGMF's SNR and the

140   GSWP3's SNR are very close (5 – 5.5) for HMF, but the former (from 6.5 to 5.5) is slightly

141   smaller than the latter (from 7.5 to 6.5) for AF. This indicates that the uncertainties in historical

142   climate data bring large discrepancies to GHMs simulations, which agrees with previous studies

143   [41].

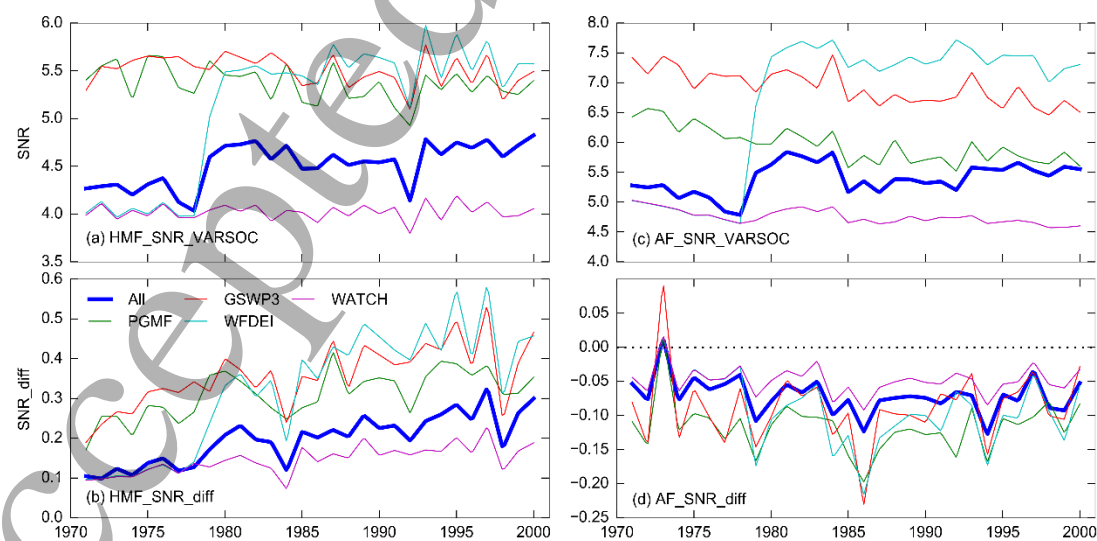144   The SNR for the simulations with human impacts is generally larger (smaller) than for the

145   naturalized simulations regarding global HMF (AF). SNR differences for global HMF (Figure

146   2b) increase over time, whereas the ensemble SNR difference ranges from 0.1 to 0.3 (2-6%);

147   the WATCH's SNR difference is the smallest, ranging from 0.1 to 0.2, while SNR differences

148   for other forcings mostly range from 0.2 to 0.5, which show relative large interannual variations.

149   SNR differences for global AF (Figure 2d) show considerable interannual variation. The all-

150   ensemble SNR difference ranges from -0.12 (2%) to zero; the WATCH's SNR difference is also

151   the smallest, and the other SNR differences mostly ranges from 0.05 to 0.15.

152

153   Figure 2. SNRs for the simulations of global mean river flows from the experiment with human impacts

154   and the differences with respect to the experiments without human impacts. (a) and (c): SNR for global

155   HMF and AF from the experiment with human impacts, respectively, (b) and (d): SNR differences for

156   global HMF AF, respectively. The blue lines indicate the SNRs (or SNR differences) across the four

157   GHMs and all forcings, while the other four color lines are SNRs across the four GHMs for the individual

158   forcings (i.e., PGMF, GSWP3, WFDEI, and WATCH).

159

160   Figure 3 shows the SNR differences between the simulations with and without human

161   impacts for the basin averaged MHMF and MAF, respectively, over the 1971-2000 period. The

162   SNR differences for HMF at basin scale shows many negative values (indicating larger

163   uncertainties), e.g. some basins in Europe, North India, and South China (Figure 3a). There are

164   generally small changes in the basins with a few reservoirs and irrigation areas, but considerable

165   positive SNR differences (lower uncertainties) are found for the Yenisey and Lena basins.

166   Lower uncertainties are also found in some major basins with great human impacts, such as the

167   Liao River and Hai River of China, the Don River of Russia, the Amu Darya River in Central

168   East, the Tigris-Euphrates River in West Asia, the Zambezi River in Africa, and the São

169   Francisco River in South America. However, only a relatively weak relationship (with a

170   correlation coefficient of 0.18) is found between the basin MHMF's SNR difference and

171   reservoir storage capacity, as shown in Figure 3c.

172   SNRs for MAF simulations with human impacts are mostly smaller than naturalized

173   simulations at basin scale. Large differences are observed in some major river basins with great

174   human impacts, such as the Chang Jiang and Huang River basins of China, the Ganges,

175   Godavari and Krishna Rivers of India, the Indus River of Pakistan, the Amu Darya River in

176   Central East, the Tigris-Euphrates River in West Asia, and the Danube River in Europe. It

177   indicates that uncertainty increases in MAF simulations with human impacts in these regions.

178   Only a few positive SNR differences (lower uncertainty) are found, e.g. in the Hai and Liao

179   River of China and the East Coast of Caspian Sea. The SNR differences for MAF are relatively

180   well related to the basin irrigation area (correlation coefficient -0.41; Figure 3d), indicating that

181   between-model uncertainty is higher for the basins with larger irrigation area.

182
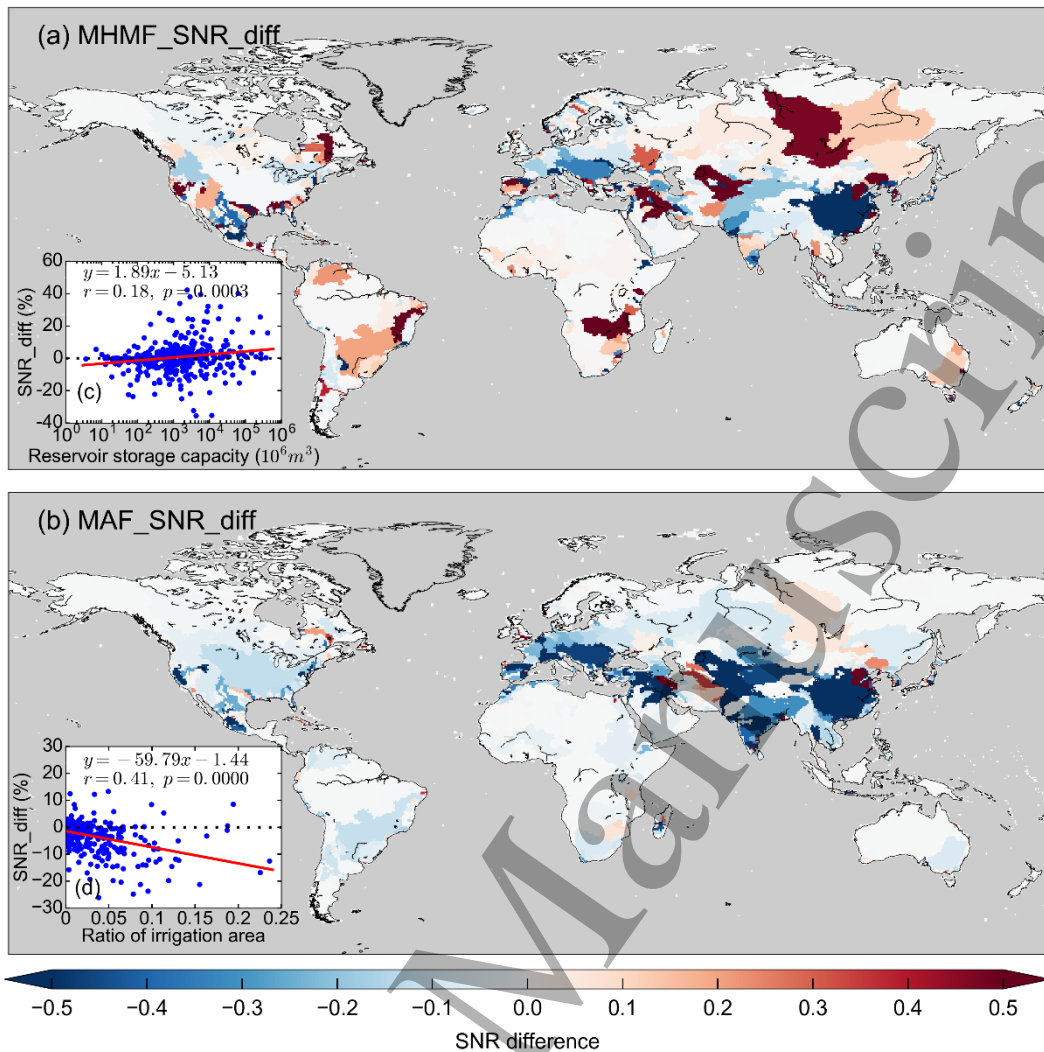
183   Figure 3. SNR difference (VARSOC – NOSOC) for basin MHMF (a) and MAF (b) simulations. SNR is

184   computed for the basin averages across all GHM-forcing combinations. Blue (red) color indicates that

185   SNRs from experiment with human impacts are smaller (larger) than SNRs from naturalized experiments.

186   That is, the blue color indicates higher uncertainty while red color indicates lower uncertainty. The inner

187   plots show the SNR differences (in %) for basin averaged MHMF versus logarithm of reservoir storage

188   capacity (c) and basin averaged MAF versus logarithm of irrigation areas (d), respectively. Basins with

189   none reservoir or irrigation area are not included in the inner plots; SNR differences above or below three

190   standard deviations are omitted.

191

192   Figure 4 shows the ratios of the SNR of human-impact-induced MAF differences to the

193   SNR of naturalized MAF at basin scale. The numerator is the SNR of MAF differences between

194   the simulations with and without human impacts. The smaller the ratio is, the larger uncertainty

195   in human impact simulations is, and vice versa. The ratios are less than one (mostly < 0.5) for

196   many basins (particularly those with numerous irrigation areas and reservoirs), that is, the SNR

197   of human-impact-induced MAF differences are obviously smaller than the MAF SNRs (see

198   Figure S3). The southern basins and the Hai River basin in China and many basins in Europe

199   with intensive human activities show very small ratios that less than 0.2. Only several basins

200   show large ratios greater than one, such as the Tarim Interior of China, the Volga of Russia, St

201   Lawrence in North America, and the Shebelli–Juba and some northern basins in Africa where

202   irrigation areas are small and reservoirs are few. It indicates that the human impact

203   simulations—i.e., the human-impact-induced MAF differences—show larger uncertainties

204   compared to the naturalized simulations in these regions.

205   Unlike the SNR differences in Figure 3, the ratios in Figure 4 are very weakly related to

206   both the fraction of irrigation area and reservoir storage capacity. Nevertheless, uncertainty in

207   irrigation—as the largest human water use—perhaps plays a key role for the small SNRs. For

208   example, the actual water withdrawal for irrigation (IRRWW) simulated by GHMs shows

209   considerable differences and is significantly underestimated compared to reported data (see
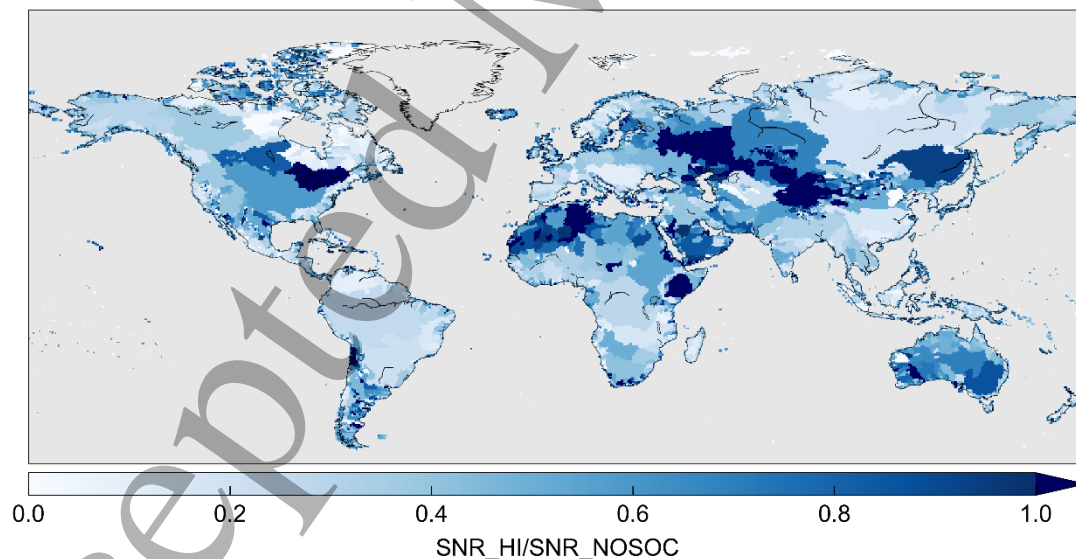
210   Figure S4).

211

212   Figure 4. The ratios of SNR of human-impact-induced MAF differences (NOSOC - VARSOC) to SNR

213   of naturalized MAF simulations. SNR_HI: the SNR of the MAF differences (NOSOC - VARSOC)

214   between the simulations without and with human impacts at basin scale; SNR_NOSOC: the SNR of

215   MAF simulations without human impacts at basin scale.

216

4. Discussion

218   The simulated river flows show large deviations with overestimation at many hydrological

219   stations compared to GRDC observations. This may be due to regional overestimation of runoff

220   generation and the underestimation of anthropogenic water uses (e.g. see Figure S4) and soil

221   water storage [42]. The between-model uncertainties are measured in terms of SNR, which are

222   larger (a bit smaller) in the annual flow (high flow) simulations with human impacts than in the

223   naturalized simulations. The differences of between-model uncertainty from the two

224   experiments are relatively small (2-4%) at global scale but are more significant for some regions.

225   Previous studies showed that human intervention (e.g. irrigation water withdrawal) largely

226   altered regional water cycle [9, 43]. The human impacts are primarily represented by

227   anthropogenic water uses (irrigation, industrial domestic, etc.) and reservoir regulation in the

228   GHMs, which increase the model complexity with respect to model structure and parameters.

229   The different model algorithms and various parameters should be responsible for the large

230   between-model uncertainties [3]. The uncertainties due to the different responses of GHMs to

231   climate input are beyond the scope of this paper. However, it is noted that the differences in

232   naturalized simulations resulted from the different responses also will influence the simulation

233   of human water uses (e.g., irrigation). Regarding to the simulations of human impacts, the

234   severely lack of water uses data primarily in developing countries should be one of the major

235   reasons leading to great deviations to observations and uncertainties among GHMs. Here, we

236   focus on the differences of the between-model uncertainties between the experiments with and

237   without human impacts, and the discussion of the potential major sources of the uncertainties

238   associated with the different parameterizations of human impacts in GHMs.

239

4.1. Uncertainties in irrigation simulations

241   The simulation of irrigation, the largest anthropogenic water use, is likely to contribute to

242   the discrepancies in the simulations of human impact by GHMs, as indicated by the relationship

243   between the SNR difference and irrigation area (Figure 3d). Irrigation water demand is usually

244   estimated as the difference of potential crop evapotranspiration and local available soil (green)

245   water. Therefore, uncertainties in IRRWW simulations are largely associated with the

246   estimation of crop evapotranspiration, soil moisture, and irrigation efficiency. Though all four

247   GHMs use the FAO Penman-Monteith equation to estimate the potential crop

248   evapotranspiration, the simulated potential water withdrawal for irrigation can be significant

249   different (see Figure S4c, d). The irrigation efficiency (the ratio of irrigation water use to the

250   total water withdrawal) varies across the GHMs (see Table S1) and may significantly influence

251   the estimation of potential and actual water withdrawal for irrigation. On the other hand, the

252   implementations of water withdrawals in GHMs may be different in several aspects, which are

253   partly responsible for the differences in IRRWW, such as the accessibility to available water for

254   a grid cell, the proportion of withdrawal from river, reservoir and groundwater, and the

255   allocation of the water supplies for different sectors from a reservoir. Hence, irrigation schemes

256   and associated parameters need to be reconciled against the observed regional conditions to

257   provide more consistent IRRWW simulations at both global and regional scales.

258

4.2. Uncertainties in reservoir simulations

259

260   Reservoir regulation scheme is critical in coupling human-induced and natural

261   hydrological changes in GHM simulations. Human impacts on hydrological processes could be

262   much more complex than the simulations in this study for they are associated with many

263   socioeconomic factors. For instance, irrigation is linked to reservoir regulation and regional

264   water allocation, while reservoir regulation rules are mostly defined by energy demand, flood

265   control, various water supplies, and even the energy and food prices [44]. The role of reservoir

266   regulation therein makes the simulation be relatively uncertain. Water losses due to evaporation

267   are particularly significant for some small reservoirs [45], which may result in uncertainty in

268   reservoir regulations since not all GHMs consider this process (Table S1).

269   The different reservoir regulation schemes inevitably bring uncertainties to river flow

270   simulations. Though the GHMs more or less take the reference of [46] or [47] in their reservoir

271   regulation development, the adapted rules are still (perhaps largely) different [15, 48, 49]. The

272   reservoir regulation may produce significantly different simulated hydrographs of the dammed

273   rivers by the GHMs [50]. Nevertheless, the uncertainty differences for both annual flow and

274   high flow are weakly related to the reservoir storage in this study. It is noted that the simulations

275 of high flow are less discrepant among GHMs in some basins (Figure 3c) with large storage

276 capacity of reservoirs (e.g. the Bratsk, Irkutsk reservoirs in the Yenisey basin and Vilyui

277 reservoirs in the Lena basin) and small irrigation areas, where the reservoir regulation greatly

278 determine the variations of downstream flow [51]. At global scale, the slightly higher

279 consistency in the high flow simulations with human impacts perhaps results from the universal

280 flood control rules in GHMs which are greatly associated with reservoir storage capacity and

281 annual average inflows.

282

4.3. Uncertainties in simulations of groundwater withdrawal

284 Groundwater withdrawal is also a key source for to the IRRWW in some regions [52].

285 However, modeling of groundwater availability remains a challenge due to the complex

286 interactions between surface water and groundwater [10, 53], and the large differences in the

287 implementation of groundwater withdrawal give rise to significant discrepancies among GHMs

288 [54]. The proportion of withdrawals from groundwater (R_{grd}) is a key parameter associated with

289 the groundwater withdrawal estimation. In current GHMs, due to insufficient historical data at

290 global scale, the proportion of groundwater withdrawal is often estimated according to water

291 use demand and surface water availability—in this case the amount of groundwater pumping

292 was often unlimited [55]—or further constrained by estimated groundwater availability and

293 historical groundwater pumping data [30, 56-58]. Leng et al. [59] showed that the calibrated

294 R_{grd} using historical census data could largely improve the simulation of irrigation amount in

295 the USA (see their Fig. 3). The PCR-GLOBWB model limits the groundwater withdrawal

296 according to its availability and the reported groundwater pumping data based on the

297 International Groundwater Resources Assessment Centre, and obtains better performances in

298 the simulations of groundwater withdrawal [30], although it may result in deviation in the

299 IRRWW estimates in regions like India and Pakistan where groundwater pumping remains

300 unreported in many parts. This studies suggested that R_{grd} could be determined from historical

301 data and is useful for improving the simulation of groundwater withdrawal, and thus reduce the

302 uncertainty among GHMs. Besides, the uncertainties in estimated water use demand, surface

303 water and groundwater availability will be propagated to the groundwater withdrawal

304 estimation. The groundwater use efficiency usually was taken the same as the surface water,

305   but it was supposed to be higher [60]. Potential uncertainty resulted from this parameter needs

306   further investigation.

307

4.4. Potential of reducing uncertainties in multimodel simulations

309   Validation and calibration of GHMs against historical observations would advance model

310   development, and are perhaps a crucial means to refine the GHMs simulations and to narrow

311   the spread therein [61, 62]. Regarding the large spread in the simulations of human water uses,

312   validations of individual sectoral water uses or hydrological components are necessary to get

313   access to more constrained and confident hydrological modelling. Though the robust

314   hydrological response to climate change in GHMs during historical period would not

315   necessarily imply good model performances—not necessarily narrow model spread either—in

316   future projections, the historical credits of GHMs would benefit the assessment presented by

317   the ranges of hydrological changes with higher confidence [3, 63].

318   On the other hand, to some degree, the discrepant GHMs simulations further call for

319   multimodel assessment rather than that based on a single model [64]. Before one can achieve

320   better performing and more consistent hydrological predictions by GHMs, advanced statistical

321   tools may be useful to improve the projections from multimodel ensembles for the assessment

322   of climate change impact. For example, the Bayesian model averaging scheme can be an

323   effective tool to obtain hydrological projections with less between-model uncertainties by

324   weighting the individual model prediction with their likelihood measures [64].

325   Modeling of the dynamics of human water uses is still a great challenge since sectoral

326   water use efficiencies are kept changing (improving) in the wake of technological developments

327   and management changes. Döll et al. [3] pointed out that the major challenges in modeling

328   human water uses in GHMs come from input data, model algorithms, scaling issues, and etc.

329   (see their Table 1). Particularly, more data of human water uses are urgently needed to further

330   understand the human disturbances on hydrological cycle and therefore to derive better

331   descriptions of them in terms of mathematical models. We noted that capturing the linkages

332   between sectors in terms of water use would also be a major challenge. Two-way coupling of

333   human water uses at different scales as well as the natural hydrological processes in GHMs is

334   perhaps necessary to mimic the connected and competitive water uses among sectors. Therefore,

335   full representation of human impacts in global hydrological modeling under climate change

336   raises the request of dynamically coupling the so-called nexus of climate-water-energy-food

337   [65, 66]. This would be more essential for future projections of water resources and uses with

338   regard of various socioeconomic scenarios [31, 67].

339

5. Conclusions

341   Global river flows simulated by four GHMs are validated and the between-model

342   uncertainties in terms of SNR are investigated with respect to the inclusion of human impacts

343   in the GHMs. The GHMs show relatively poor performances with considerable between-model

344   uncertainties in the simulations of annual (AF) and high flow (HMF). Main conclusions can be

345   drawn as follows.

346   (1) Over the historical period (1971-2000), the GHMs show limitations in modeling AF

347   and HMF at many stations—particularly for those from small basins, while relatively better

348   performance is observed at many large basins. The multimodel ensemble means fit better to

349   observations than individual models.

350   (2) With consideration of human impacts (irrigation and reservoirs in this paper), the

351   between-model uncertainties of simulated annual flow are higher (~2% on average globally in

352   terms of SNR) compared to those from naturalized simulations, but are lower (2~4% globally)

353   for the simulated high flow. The uncertainty differences are largest in most areas of Asia and

354   northern countries of the Mediterranean Sea, and they appear to be significantly related to the

355   fractional irrigation area of river basins.

356   (3) The consistency of human impacts simulations between GHMs is much less

357   pronounced than in the naturalized simulations, probably due to differences in the

358   parameterizations of human impacts (especially the irrigation).

359   The large uncertainties in human impact parameterizations put forward the need for further

360   development of GHMs (not only for the models used in this paper) to reduce between-model

361   uncertainties associated with irrigation and reservoir regulation. It is the first quantitative

362   investigation of between-model uncertainty resulting from the inclusion of human impact

363   parameterizations, and the quantitative method may be used to examine uncertainty caused by

364 other parameterizations in GHMs. In this study, we emphasize that calibration of GHMs

365 including representations of the anthropogenic effects on the water cycle are essential for global

366 hydrological modeling of a changing environment. Reconciliation of human water uses

367 schemes and associated parameters in GHMs with global and regional observations would

368 facilitate improvement of human impact parameterizations. Ensemble prediction approaches

369 are promising tools for reducing uncertainty in model intercomparison projects, and would

370 benefit future hydrological projections in assessment of climate change impact.

371

372 Acknowledgement

378

379 References

380 [1] Vörösmarty, C. J., and D. Sahagian (2000), Anthropogenic Disturbance of the Terrestrial

381 Water Cycle, BioScience, 50(9), 753-765, doi: 10.1641/0006-

382 3568(2000)050[0753:adottw]2.0.co;2.

383 [2] Milly, P. C. D., J. Betancourt, M. Falkenmark, R. M. Hirsch, Z. W. Kundzewicz, D. P.

384 Lettenmaier, and R. J. Stouffer (2008), Stationarity Is Dead: Whither Water Management?,

385 Science, 319(5863), 573-574.

386 [3] Döll, P., H. Douville, A. Güntner, H. Müller Schmied, and Y. Wada (2016), Modelling

387 Freshwater Resources at the Global Scale: Challenges and Prospects, Surv. Geophys., 37(2),

388 195-221, doi: 10.1007/s10712-015-9343-1.

389 [4] Müller Schmied, H., et al. (2016), Variations of global and continental water balance

390 components as impacted by climate forcing uncertainty and human water use, Hydrol. Earth

391 Syst. Sci., 20(7), 2877-2898, doi: 10.5194/hess-20-2877-2016.

392 [5] Döll, P., and S. Siebert (2002), Global modeling of irrigation water requirements, Water

393   Resour. Res., 38(4), 8-1-8-10, doi: 10.1029/2001WR000355.

394   [6] Oki, T., and S. Kanae (2006), Global Hydrological Cycles and World Water Resources,

395   Science, 313(5790), 1068-1072, doi: 10.1126/science.1128845.

396   [7] Gerten, D., S. Rost, W. von Bloh, and W. Lucht (2008), Causes of change in 20th century

397   global river discharge, Geophys. Res. Lett., 35(20), L20405, doi: 10.1029/2008GL035258.

398   [8] Wada, Y., L. P. H. van Beek, N. Wanders, and M. F. P. Bierkens (2013), Human water

399   consumption intensifies hydrological drought worldwide, Environ. Res. Lett., 8(3), 034036, doi:

400   10.1002/grl.50686.

401   [9] Haddeland, I., et al. (2014), Global water resources affected by human interventions and

402   climate change, Proceedings of the National Academy of Sciences, 111(9), 3251-3256, doi:

403   10.1073/pnas.1222475110.

404   [10] Pokhrel, Y. N., S. Koirala, P. J. F. Yeh, N. Hanasaki, L. Longuevergne, S. Kanae, and T.

405   Oki (2015), Incorporation of groundwater pumping in a global Land Surface Model with the

406   representation   of   human   impacts,   Water   Resour.   Res.,   51(1),   78-96,   doi:

407   10.1002/2014WR015602.

408   [11] Tang, Q., and T. Oki (Editors) (2016), Terrestrial Water Cycle and Climate Change: Natural

409   and Human-Induced Impacts, American Geophysical Union (AGU) Geophysical Monograph

410   Series, Vol 221, 252 pp., John Wiley & Sons, Hoboken, New Jersey.

411   [12] Hanasaki, N., S. Kanae, T. Oki, K. Masuda, K. Motoya, N. Shirakawa, Y. Shen, and K.

412   Tanaka (2008), An integrated model for the assessment of global water resources – Part 1:

413   Model description and input meteorological forcing, Hydrol. Earth Syst. Sci., 12(4), 1007-1025,

414   doi: 10.5194/hess-12-1007-2008.

415   [13] Tang, Q., T. Oki, S. Kanae, and H. Hu (2008), Hydrological cycles change in the Yellow

416   River Basin during the last half of the twentieth century, J. Climate, 21(8), 1790-1806, doi:

417   10.1175/2007JCLI1854.1.

418   [14] Wisser, D., S. Frolking, E. M. Douglas, B. M. Fekete, A. H. Schumann, and C. J.

419   Vörösmarty (2010), The significance of local water resources captured in small reservoirs for

420   crop   production   –   A   global-scale   analysis,   J.   Hydrol.,   384(3–4),   264-275,   doi:

421   10.1016/j.jhydrol.2009.07.032.

422   [15] Biemans, H., I. Haddeland, P. Kabat, F. Ludwig, R. W. A. Hutjes, J. Heinke, W. von Bloh,

423　　and D. Gerten (2011), Impact of reservoirs on river discharge and irrigation water supply during

424　　the 20th century, Water Resour. Res., 47(3), W03509, doi: 10.1029/2009WR008929.

425　　[16] Pokhrel, Y., N. Hanasaki, S. Koirala, J. Cho, P. J. F. Yeh, H. Kim, S. Kanae, and T. Oki

426　　(2011), Incorporating anthropogenic water regulation modules into a land surface model, J.

427　　Hydrometeor, 13(1), 255-269, doi: 10.1175/JHM-D-11-013.1.

428　　[17] Wada, Y., L. P. H. van Beek, D. Viviroli, H. H. Dürr, R. Weingartner, and M. F. P. Bierkens

429　　(2011), Global monthly water stress: 2. Water demand and severity of water stress, Water

430　　Resour. Res., 47(7), W07518, doi: 10.1029/2010WR009792.

431　　[18] Voisin, N., H. Li, D. Ward, M. Huang, M. Wigmosta, and L. R. Leung (2013), On an

432　　improved sub-regional water resources management representation for integration into earth

433　　system models, Hydrol. Earth Syst. Sci., 17(9), 3605-3622, doi: 10.5194/hess-17-3605-2013.

434　　[19] Duan, Q., et al. (2006), Model Parameter Estimation Experiment (MOPEX): An overview

435　　of science strategy and major results from the second and third workshops, J. Hydrol., 320(1–

436　　2), 3-17, doi: 10.1016/j.jhydrol.2005.07.031.

437　　[20] Haddeland, I., et al. (2011), Multimodel estimate of the global terrestrial water balance:

438　　Setup and first results, J. Hydrometeor, 12(5), 869-884, doi: 10.1175/2011JHM1324.1.

439　　[21] Prudhomme, C., et al. (2014), Hydrological droughts in the 21st century, hotspots and

440　　uncertainties from a global multimodel ensemble experiment, Proceedings of the National

441　　Academy of Sciences, 111(9), 3262-3267, doi: 10.1073/pnas.1222473110.

442　　[22] Schewe, J., et al. (2014), Multimodel assessment of water scarcity under climate change,

443　　Proc. Nat. Acad. Sci. U.S.A., 111(9), 3245-3250, doi: 10.1073/pnas.1222460110.

444　　[23] Elliott, J., et al. (2014), Constraints and potentials of future irrigation water availability on

445　　agricultural production under climate change, Proc. Nat. Acad. Sci. U.S.A., 111(9), 3239-3244,

446　　doi: 10.1073/pnas.1222474110.

447　　[24] Tang, Q., T. Oki, and S. Kanae (2006), A distributed biosphere hydrological model (DBHM)

448　　for large river basin, Annual Journal of Hydraulic Engineering, 50, 37-42.

449　　[25] Tang, Q., T. Oki, S. Kanae, and H. Hu (2007), The influence of precipitation variability

450　　and partial irrigation within grid cells on a hydrological simulation, J. Hydrometeor, 8(3), 499-

451　　512, doi: 10.1175/jhm589.1, 2007.

452　　[26] Liu, X., Q. Tang, X. Zhang, and G. Leng (2016), Modeling the role of vegetation in

453   hydrological responses to climate change, in Terrestrial Water Cycle and Climate Change:

454   Natural and Human-Induced Impacts, edited by Q. Tang and T. Oki, John Wiley & Sons,

455   Hoboken, New Jersey.

456   [27] Hanasaki, N., S. Kanae, T. Oki, K. Masuda, K. Motoya, N. Shirakawa, Y. Shen, and K.

457   Tanaka (2008), An integrated model for the assessment of global water resources – Part 2:

458   Applications and assessments, Hydrol. Earth Syst. Sci., 12(4), 1027-1037, doi: 10.5194/hess-

459   12-1027-2008.

460   [28] Rost, S., D. Gerten, A. Bondeau, W. Lucht, J. Rohwer, and S. Schaphoff (2008),

461   Agricultural green and blue water consumption and its influence on the global water system,

462   Water Resour. Res., 44(9), W09405, doi: 10.1029/2007WR006331.

463   [29] Schaphoff, S., U. Heyder, S. Ostberg, D. Gerten, J. Heinke, and W. Lucht (2013),

464   Contribution of permafrost soils to the global carbon budget, Environ. Res. Lett., 8(1), 014026.

465   [30] Wada, Y., D. Wisser, and M. F. P. Bierkens (2014), Global modeling of withdrawal,

466   allocation and consumptive use of surface water and groundwater resources, Earth Syst.

467   Dynam., 5(1), 15-40, doi: 10.5194/esd-5-15-2014.

468   [31] Wada, Y., et al. (2016), Modeling global water use for the 21st century: the Water Futures

469   and Solutions (WFaS) initiative and its approaches, Geosci. Model Dev., 9(1), 175-222, doi:

470   10.5194/gmd-9-175-2016.

471   [32] Sheffield, J., G. Goteti, and E. F. Wood (2006), Development of a 50-year high-resolution

472   global dataset of meteorological forcings for land surface modeling, J. Climate, 19(13), 3088-

473   3111, doi: 10.1175/jcli3790.1.

474   [33] Dirmeyer, P. A., X. Gao, M. Zhao, Z. Guo, T. Oki, and N. Hanasaki (2006), GSWP-2:

475   Multimodel analysis and implications for our perception of the land surface, Bull. Am. Meteorol.

476   Soc., 87(10), 1381-1397, doi: doi:10.1175/BAMS-87-10-1381.

477   [34] Weedon, G. P., G. Balsamo, N. Bellouin, S. Gomes, M. J. Best, and P. Viterbo (2014), The

478   WFDEI meteorological forcing data set: WATCH forcing data methodology applied to ERA-

479   Interim reanalysis data, Water Resour. Res., 50(9), 7505-7514, doi: 10.1002/2014WR015638.

480   [35] Weedon, G. P., S. Gomes, P. Viterbo, W. J. Shuttleworth, E. Blyth, H. Österle, J. C. Adam,

481   N. Bellouin, O. Boucher, and M. Best (2011), Creation of the WATCH forcing data and its use

482   to assess global and regional reference crop evaporation over land during the twentieth century,

483   J. Hydrometeor, 12(5), 823-848, doi: 10.1175/2011jhm1369.1.

484   [36] Portmann, F. T., S. Siebert, and P. Döll (2010), MIRCA2000—Global monthly irrigated

485   and rainfed crop areas around the year 2000: A new high-resolution data set for agricultural and

486   hydrological   modeling,   Global   Biogeochem.   Cycles,   24(1),   GB1011,   doi:

487   10.1029/2008GB003435.

488   [37] Fader, M., S. Rost, C. Müller, A. Bondeau, and D. Gerten (2010), Virtual water content of

489   temperate cereals and maize: Present and potential future patterns, J. Hydrol., 384(3–4), 218-

490   231, doi: 10.1016/j.jhydrol.2009.12.011.

491   [38] Lehner, B., et al. (2011), High-resolution mapping of the world's reservoirs and dams for

492   sustainable river-flow management, Frontiers in Ecology and the Environment, 9(9), 494-502,

493   doi: 10.1890/100125.

494   [39] Döll, P., and B. Lehner (2002), Validation of a new global 30-min drainage direction map,

495   J. Hydrol., 258(1–4), 214-231, doi: 10.1016/S0022-1694(01)00565-0.

496   [40] GRDC (2015): Long-Term Mean Monthly Discharges and Annual Characteristics of

497   GRDC Stations / Online provided by the Global Runoff Data Centre of WMO. 2015 ed.

498   Koblenz: Federal Institute of Hydrology (BfG), [Date of retrieval: 2015-10-22].

499   [41] Müller Schmied, H., S. Eisner, D. Franz, M. Wattenbach, F. T. Portmann, M. Flörke, and

500   P. Döll (2014), Sensitivity of simulated global-scale freshwater fluxes and storages to input data,

501   hydrological model structure, human water use and calibration, Hydrol. Earth Syst. Sci., 18(9),

502   3511-3538, doi: 10.5194/hess-18-3511-2014.

503   [42] Döll, P., M. Fritsche, A. Eicker, and H. Müller Schmied (2014), Seasonal water storage

504   variations as impacted by water abstractions: Comparing the output of a global hydrological

505   model with GRACE and GPS observations, Surv. Geophys., 35(6), 1311-1331, doi:

506   10.1007/s10712-014-9282-2.

507   [43] Zhou, T., B. Nijssen, H. Gao, and D. P. Lettenmaier (2015), The contribution of reservoirs

508   to global land surface water storage variations, J. Hydrometeor., 17(1), 309-325, doi:

509   10.1175/JHM-D-15-0002.1.

510   [44] Voisin, N., L. Liu, M. Hejazi, T. Tesfa, H. Li, M. Huang, Y. Liu, and L. R. Leung (2013),

511   One-way coupling of an integrated assessment model and a water resources model: evaluation

512   and implications of future changes over the US Midwest, Hydrology and Earth System Sciences,

513   17(11), 4555-4575, doi: 10.5194/hess-17-4555-2013.

514   [45] Fekete, B. M., D. Wisser, C. Kroeze, E. Mayorga, L. Bouwman, W. M. Wollheim, and C.

515   Vörösmarty (2010), Millennium Ecosystem Assessment scenario drivers (1970–2050): Climate

516   and   hydrological   alterations,   Global   Biogeochem.   Cycles,   24(4),   GB0A12,   doi:

517   10.1029/2009GB003593.

518   [46] Hanasaki, N., S. Kanae, and T. Oki (2006), A reservoir operation scheme for global river

519   routing models, J. Hydrol., 327(1–2), 22-41, doi: 10.1016/j.jhydrol.2005.11.011.

520   [47] Haddeland, I., D. P. Lettenmaier, and T. Skaugen (2006), Effects of irrigation on the water

521   and energy balances of the Colorado and Mekong river basins, J. Hydrol., 324(1-4), 210-223,

522   doi: DOI 10.1016/j.jhydrol.2005.09.028.

523   [48] van Beek, L. P. H., Y. Wada, and M. F. P. Bierkens (2011), Global monthly water stress: 1.

524   Water   balance   and   water   availability,   Water   Resour.   Res.,   47(7),   W07517,   doi:

525   10.1029/2010WR009791.

526   [49] Liu, X., Q. Tang, N. Voisin, and H. Cui (2016), Projected impacts of climate change on

527   hydropower potential in China, Hydrol. Earth Syst. Sci., 20(8), 3343-3359, doi: 10.5194/hess-

528   20-3343-2016.

529   [50] Masaki, Y., N. Hanasaki, H. Biemans, H. Müller Schmied, Q. Tang, Y. Wada, S. N. Gosling,

530   K. Takahashi and Y. Hijioka, (2017) Intercomparison of global river discharge simulations

531   focusing on dam operation - Part II: Multiple models analysis in two case-study river basins,

532   Missouri-Mississippi and Green-Colorado, Environ. Res. Lett., (accepted).

533   [51] Adam, J. C., I. Haddeland, F. Su, and D. P. Lettenmaier (2007), Simulation of reservoir

534   influences on annual and seasonal streamflow changes for the Lena, Yenisei, and Ob' rivers, J.

535   Geophys. Res., 112(D24).

536   [52] Tang, Q., H. Hu, and T. Oki (2007), Groundwater recharge and discharge in a hyperarid

537   alluvial plain (Akesu, Taklimakan Desert, China), Hydrol. Processes, 21(10), 1345-1353, doi:

538   10.1002/hyp.6307.

539   [53] Wu, B., Y. Zheng, Y. Tian, X. Wu, Y. Yao, F. Han, J. Liu, and C. Zheng (2014), Systematic

540   assessment of the uncertainty in integrated surface water-groundwater modeling based on the

541   probabilistic   collocation   method,   Water   Resour.   Res.,   50(7),   5848-5865,   doi:

542   10.1002/2014WR015366.

543 [54] Wada, Y. (2016), Modeling groundwater depletion at regional and global scales: Present

544 state and future prospects, Surv. Geophys., 37(2), 419-451, doi: 10.1007/s10712-015-9347-x.

545 [55] Hanasaki, N., T. Inuzuka, S. Kanae, and T. Oki (2010), An estimation of global virtual

546 water flow and sources of water withdrawal for major crops and livestock products using a

547 global hydrological model, J. Hydrol., 384(3–4), 232-244, doi: 10.1016/j.jhydrol.2009.09.028.

548 [56] Wada, Y., and L. Heinrich (2013), Assessment of transboundary aquifers of the world—

549 vulnerability arising from human water use, Environ. Res. Lett., 8(2), 024003, doi:

550 10.1088/1748-9326/8/2/024003.

551 [57] Wada, Y., L. P. H. van Beek, and M. F. P. Bierkens (2012), Nonsustainable groundwater

552 sustaining irrigation: A global assessment, Water Resour. Res., 48(6), W00L06, doi:

553 10.1029/2011WR010562.

554 [58] Wada, Y., L. P. H. van Beek, C. M. van Kempen, J. W. T. M. Reckman, S. Vasak, and M.

555 F. P. Bierkens (2010), Global depletion of groundwater resources, Geophys. Res. Lett., 37(20),

556 L20402, doi: 10.1029/2010GL044571.

557 [59] Leng, G., M. Huang, Q. Tang, H. Gao, and L. R. Leung (2014), Modeling the effects of

558 groundwater-fed irrigation on terrestrial hydrology over the conterminous United States, J.

559 Hydrometeor, 15(3), 957-972, doi: 10.1175/jhm-d-13-049.1.

560 [60] Döll, P., H. Müller Schmied, C. Schuh, F. T. Portmann, and A. Eicker (2014), Global-scale

561 assessment of groundwater depletion and related groundwater abstractions: Combining

562 hydrological modeling with information from well observations and GRACE satellites, Water

563 Resour. Res., 50(7), 5698-5720, doi: 10.1002/2014WR015595

564 [61] Döll, P., and H. M. Schmied (2012), How is the impact of climate change on river flow

565 regimes related to the impact on mean annual runoff? A global-scale analysis, Environ. Res.

566 Lett., 7(1), 014037.

567 [62] Nearing, G. S., D. M. Mocko, C. D. Peters-Lidard, S. V. Kumar, and Y. Xia (2016),

568 Benchmarking NLDAS-2 soil moisture and evapotranspiration to separate uncertainty

569 contributions, J. Hydrometeor, 17(3), 745-759, doi: 10.1175/JHM-D-15-0063.1.

570 [63] Greuell, W., J. C. M. Andersson, C. Donnelly, L. Feyen, D. Gerten, F. Ludwig, G. Pisacane,

571 P. Roudier, and S. Schaphoff (2015), Evaluation of five hydrological models across Europe and

572 their suitability for making projections under climate change, Hydrol. Earth Syst. Sci. Discuss.,

573   2015, 10289-10330, doi: 10.5194/hessd-12-10289-2015.

574   [64] Duan, Q., N. K. Ajami, X. Gao, and S. Sorooshian (2007), Multi-model ensemble

575   hydrologic prediction using Bayesian model averaging, Adv. Water Res., 30(5), 1371-1386, doi:

576   10.1016/j.advwatres.2006.11.014.

577   [65] Conway, D., et al. (2015), Climate and southern Africa's water-energy-food nexus, Nature

578   Clim. Change, 5(9), 837-846, doi: 10.1038/nclimate2735.

579   [66] Smajgl, A., J. Ward, and L. Pluschke (2016), The water–food–energy Nexus – Realising a

580   new paradigm, J. Hydrol., 533, 533-540, doi: 10.1016/j.jhydrol.2015.12.033.

581   [67] Yin, Y., Q. Tang, X. Liu, and X. Zhang (2016), Water scarcity under various socio-

582   economic pathways and its potential effects on food production in the Yellow River Basin,

583   Hydrol. Earth Syst. Sci. Discuss., doi: 10.5194/hess-2016-188.